Original Paper

phys. stat. sol. (b) **244**, No. 4, 1181–1187 (2007) / **DOI** 10.1002/pssb.200674503

Magnetic response of split ring resonators at terahertz frequencies

Costas M. Soukoulis[*, 1, 2], **Thomas Koschny**[1], **Jiangfeng Zhou**[1], **Maria Kafesaki**[2], and **Eleftherios N. Economou**[3]

[1] Ames Laboratory and Department of Physics and Astronomy, Iowa State University, Ames, Iowa 50011, USA
[2] Institute of Electronic Structure and Laser – FORTH, and Department of Materials Science and Technology, University of Crete, Greece
[3] Institute of Electronic Structure and Laser – FORTH, and Department of Physics, University of Crete, Greece

Received 19 September 2006, revised 30 December 2006, accepted 2 January 2007
Published online 22 March 2007

PACS 41.20.Jb, 42.25.Bs, 42.70.Qs, 73.20.Mf

We investigate numerically the electric and the magnetic response of the split-ring resonators (SRRs) for different electromagnetic (EM) field polarization and propagation directions. We have studied the current density J of circular and rectangular SRRs at THz frequencies. At low frequencies, J is confined to the edges of the SRRs, while at high frequencies J is all over the width of the wire. The diamagnetic response of the SRRs is also examined. Finally, the role of losses and the magnetic resonance frequency are studied as the size of the SRRs becomes less than 100 nm.

1 Introduction

The idea of left-handed (LH) materials, i.e. materials with both negative electrical permittivity (ε) and magnetic permeability (μ), where the electric field (E), magnetic field (B), and wave vector ($\boldsymbol{k}$) form a left-handed coordinate system, was developed by Veselago [1] decades ago. However, it was only recently that such materials were investigated experimentally [2–4], despite their rich physics and the large number of associated potential applications, e.g. in the formation of a perfect lens [5]. The first experimental realization of LH-materials was achieved by separately constructing $\varepsilon < 0$ and $\mu < 0$ components, and then by combining them together forming a left-handed material (LHM). Although it has been well known how to obtain a $\varepsilon < 0$ material easily (e.g. using wire arrays [6]), the realization of $\mu < 0$ response (especially at high frequencies) has been a challenge, due to the absence of naturally occurring magnetic materials with negative μ. The possibility of the realization of a $\mu < 0$ material was predicted in 1999 by Pendry et al., who suggested a design made of concentric metallic ring with gaps, called split ring resonators (SRRs) which exhibits a $\mu < 0$ regime in the vicinity of the magnetic resonance frequency ω_{m} of the SRR structure [7].

In the past few years there has been ample proof for the existence of Negative Index Materials (NIMs) in the GHz frequency range. A lot of groups were able to fabricate [2, 8–10] NIMs with an index of refraction $n = -1$ with losses of less than 1 dB/cm. Recently different groups observed indirectly [11–14] negative μ at the THz region. In most of the THz experiments [11, 13, 14] only one layer of SRRs were fabricated on a substrate and the transmission, T, was measured only for propagation perpendicular to

[*] Corresponding author: e-mail: soukoulis@ameslab.gov

the plane of the SRRs, exploiting the coupling of the electric field to the magnetic resonance of the SRR via asymmetry [15]. This way it is not possible to drive the magnetic permeability negative. Also, no negative n with small imaginary part has been observed yet at the THz region [16, 17]. One reason is that is very difficult to measure with the existing topology of SRRs and continuous wires both the transmission, T, and reflection, R, along the direction parallel to the plane of the SRRs. So there is a need for alternative, improved and simplified designs that can be easily fabricated and experimentally characterized. This was recently achieved in the GHz region [18, 19] and in the THz region [16, 17] by the use of finite length wires and the fish-net topology.

In this manuscript, we will present results of the magnetic response of SRRs as the size of SRRs reduce in size. As shown Zhou et. al. [20], scaling (ω_m vs $1/L$) is obeyed for $L > 500$ nm, while for smaller L, the magnetic resonance frequency saturates. We have systematically studied the current density as well as the magnetic response of the SRRs. We have also calculated the losses of the SRRs as their size decreases. It is found that losses increase as the size of the SRRs decreases. We have also shown that the effective magnetic permeability $\mu(\omega)$ does not approach 1 as $\omega \to 0$ and $\omega \to \infty$. This is due to the diamagnetic response of the SRRs. We present numerical results which support this conclusion. One way to increase the magnetic resonance frequency ω_m is to introduce four-cut SRRs [20]. We have systematically studied ω_m versus the size of the four-cut SRRs. As in the case of the one-cut SRRs, scaling ($\omega_m \sim 1/L$) is obeyed for $L > 500$ nm while for $L < 500$ nm saturation of ω_m is also obtained. Using the retrieval procedure [21, 22] we have calculated $\mu(\omega)$, both the real and imaginary part of $\mu(\omega)$, for the one-cut and four-cut SRRs. As the size of the SRR (for both the one-cut and four-cut SRRs) decreases the resonance of $\mu(\omega)$ gets weaker and the imaginary part of $\mu(\omega)$ gets stronger. This also means that the losses become larger as the size of the SRR gets smaller. The paper is organized as follows: In Section II we present the results for one-cut SRRs. In Section III we present the results for four-cut SRRs. Finally in Section IV we give our conclusions.

2 Scaling, saturation of ω_m of the one-cut SRRs and their magnetic response

We simulate single-ring SRRs similar to the experimental samples previously employed in the 200 THz frequency range [13] for near infrared and optical frequencies using the commercial finite-element based PDE solver COMSOL Multiphysics. The propagation direction of the incident EM field is along the plane of the SRR, with the electric field parallel to the sides of the SRR that do not have a cut, while the magnetic field is perpendicular to the plane of the SRR. In Fig. 1, we show the results of our simulations for the resonance frequency ω_m versus the inverse size of the unit cell.

For large enough sizes ($L > 500$ nm) ω_m scales as $1/L$, while for smaller SRR unit cells ($L < 400$ nm) ω_m saturates [20].

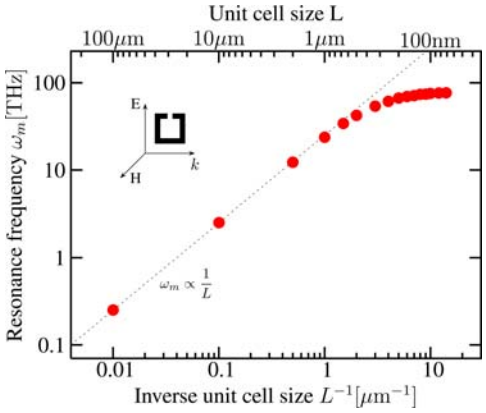

Fig. 1 (online colour at: www.pss-b.com) Scaling of the magnetic resonance frequency of the single-cut SRR with the inverse unit size is shown. The parameters of single-cut SRR are given by length $l = 0.8L$, width $l = 0.1L$, thickness of the metal $t = 0.05L$ and gap-size $g = 0.02L$. The linear scaling $\omega_m \propto 1/L$ at low frequencies (large unit cells) breaks down at around 100 THz.

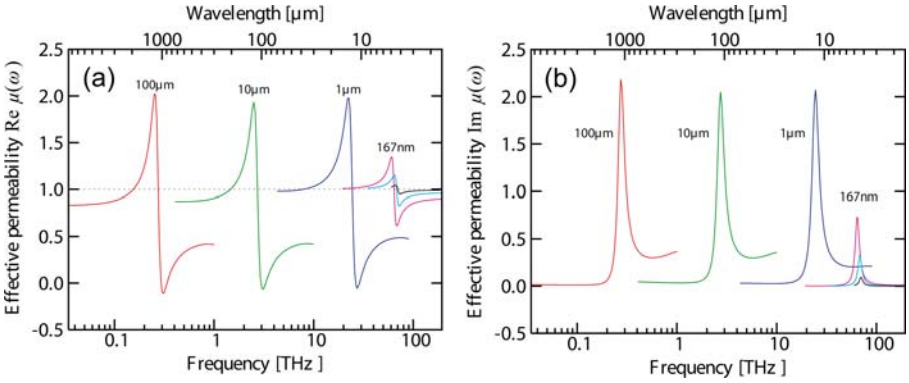

Fig. 2 (online colour at: www.pss-b.com) Real part (a) and imaginary part (b) of the resonant effective permeability $\mu(\omega)$ are shown for a single-gap SRR as function of frequency for different sizes L of the SRR unit cell: $L = 100$ μm (red), 10 μm (green), 1 μm (blue), 167 nm (pink), 100 nm (turquoise) and 50 nm (black).

The saturation of ω_m at high frequencies is due to the extra inductance, L_e, that the electrons acquire as the SRR unit cell gets smaller [20]. L_e scales like $\sim 1/L$, while the geometric inductance due to the shape of the SRR, L_m, scales $\sim L$ and the capacitance, C, contributed by the cut in the SRR rings behaves $\sim 1/L$. So the magnetic resonance frequency $\omega_m = 1/\sqrt{(L_e + L_m)\,C} = 1/\sqrt{c_1 + c_2 L^2}$. Thus as $L \to 0$, ω_m saturates to a constant value.

In Fig. 2, we present the real and the imaginary part of the effective magnetic permeability $\mu(\omega)$ for the different sizes of the unit cell of single-cut SRRs. Notice that the resonant response in $\mu(\omega)$ gets weaker as the size of the system decreases. Notice also that the resonant response of the single-cut SRR approaches unity for high frequencies. The smallest size we have studied numerically is $L = 50$ nm. Also the peak in the imaginary part of $\mu(\omega)$ gets smaller, and its width increases as the size of the single-cut SRR gets smaller. The same is true for the magnetic loss tangent, which is given as Im $\mu(\omega)$/Re $\mu(\omega)$ and shown in Fig. 3.

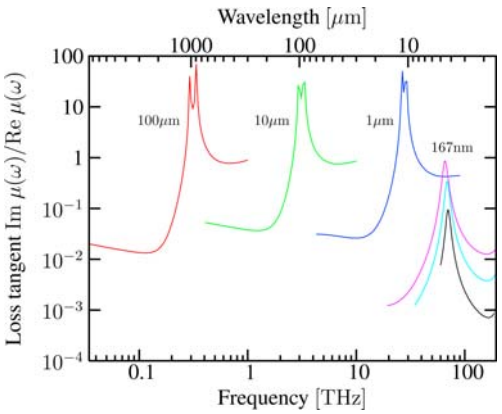

Fig. 3 (online colour at: www.pss-b.com) Magnetic loss tangent Im $(\mu(\omega))$/Re $(\mu(\omega))$ is shown for a single-gap SRR as a function of frequency for different sizes L of the SRR unit cell: $L = 100$ μm (red), 10 μm (green), 1 μm (blue), 167 nm (pink), 100 nm (turquoise) and 50 nm (black).

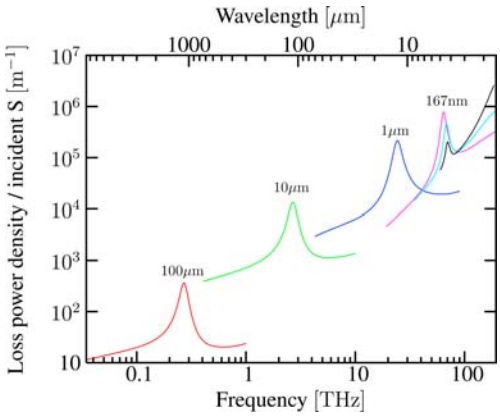

Fig. 4 (online colour at: www.pss-b.com) Loss power density per incident power flow density (Poynting vector) is shown across the magnetic resonance for the different single-cut SRR sizes form Fig. 1.

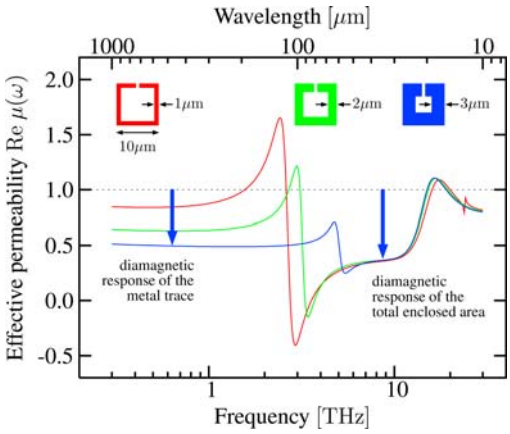

Fig. 5 (online colour at: www.pss-b.com) Real part of the effective magnetic permeability Re ($\mu(\omega)$) is shown around the magnetic resonance for a fixed SRR size of 10 μm and different widths of the metallic ring. Note the diamagnetic response of the metal area (left, below resonance) and the total enclosed ring area (right, above resonance).

A better way to assess the role of the losses in the SRR is to calculate directly the loss power density, which describes the ohmic loss in the metal and is given by $P = \sigma E^2 + (\partial \boldsymbol{D}/\partial t)\cdot \boldsymbol{E}$. In Fig. 4, we present the loss power density normalized to the incident Poynting vector $\boldsymbol{S}$. Notice that the loss density is getting larger as the size of the SRR decreases.

Another curious effect shown in Fig. 2 is that $\mu(\omega)$ does not approach unity for low frequencies or for high frequencies. In Fig. 5, we show the real part of the effective permeability $\mu(\omega)$ for three different SRRs. The size, $L = 10$ μm, is the same for all three cases. The only difference is the width of the SRR ring metal. At low frequencies $\mu(\omega)$ deviates from unity and as the width of the SRR metal increases $\mu(\omega)$ approaches 0.5. However, in the high frequency regions, just below the peak at 20 THz $\mu(\omega)$ is independent of the width of the SRR metal. To understand this behavior, we have systematically studied the current densities, as well as the component of the magnetic field perpendicular to the SRR plane for the single-cut SRR at low and high frequencies. In Fig. 6a, we plot the current density of the single-cut SRR of 10 μm size at 300 GHz (i.e. below the resonance).

Notice that the current density is non-zero only at the outer and inner edge of the circular SRR. The current direction at the outer side is clockwise, while at the inner side of the SRR it is counterclockwise. In the gap region of the SRR the current density is in opposite directions. There is no current circulating inside the metallic ring at 300 GHz. This is the diamagnetic response of the single-cut SRR. The diamagnetic response can be easily seen in Fig. 7a, where we plot the z-component of the magnetic field,

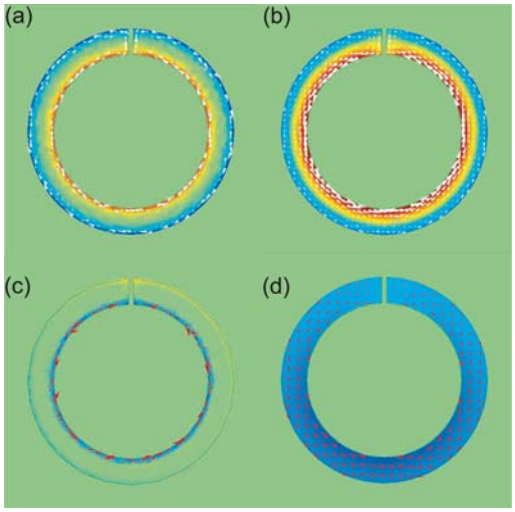

Fig. 6 (online colour at: www.pss-b.com) Current distribution inside the SRR is shown for the diamagnetic response below the magnetic response at (a) 300 GHz (SRR size L = 10 μm); and (b) 30 THz (SRR size L = 100 nm); as well as for the resonant response of (c) 3 THz (L = 10 μm), and (d) 116 THz (L = 100 nm).

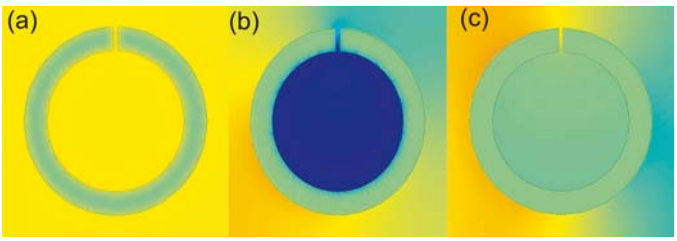

Fig. 7 (online colour at: www.pss-b.com) Magnetic field component perpendicular to the SRR plane is shown in the SRR plane for a frequency of (a) 300 GHz, below the resonance; (b) 3 THz, at the resonance; and (c) 13 THz, above the resonance. Note the negative magnetic response in (b) and the two different limits of diamagnetic response in (a) and (c). The size of the SRR is L = 10 μm. Yellow color represents positive, blue negative and green zero intensity field.

B_z. Notice that $B_z = 0$ (green color) inside the metallic ring, as expected from the exclusion of the magnetic field from the interior of the metal due to the diamagnetic response.

In Fig. 7c, we plot B_z for the same size SRR ($L = 10$ μm) but at higher frequency (13 THz, above the resonance). At 13 THz $\mu(\omega) \approx 0.5$, independent of the width of the metallic ring of the SRR. As can be seen from Fig. 7c, $B_z = 0$ not only at the metallic ring of the SRR but also throughout the enclosed area of the SRR. So the magnetic field is excluded from the area of the SRR, and this is the reason that $\mu(\omega) \approx 0.5$ independent of the width of the metallic ring. Figure 7b shows the strong negative magnetic response of the SRR slightly above the resonance frequency ω_m (3 THz).

In Fig. 6b we show the current distribution responsible for the diamagnetic response for a smaller SRR with $L = 100$ nm at 30 THz (below the resonance). Here the current extends deep into the metal of the ring. Figure 6c and 6d show the current distribution directly at the resonance frequency for the 10 μm SRR (at 3THz) and the 10 μm SRR (at 116THz), respectively.

For the low frequency case the resonant current (which overshadows the much weaker diamagnetic currents) only flows in a thin layer (skin-depth) at the inner edge of the SRR.

At high frequency (or small SRR size), the skin-depth as well as the resonance frequency starts to saturate (due to the finite electron mass), which leads to an increasing ratio of skin-depth over SRR size, hence a deeper penetration of the current into the metal. At 116 THz (Fig. 6d) the resonant current is already homogeneously distributed over the whole cross-section of the SRR ring.

3 Four-cut SRR give negative μ at optical frequencies

As we discussed in Ref. [20] the 4-cut SRR retains the negative Re ($\mu(\omega)$) region for higher frequencies (up to about 550 THz). As one can see from Fig. 8, the resonance frequency, ω_m, of the 4-cut SRR

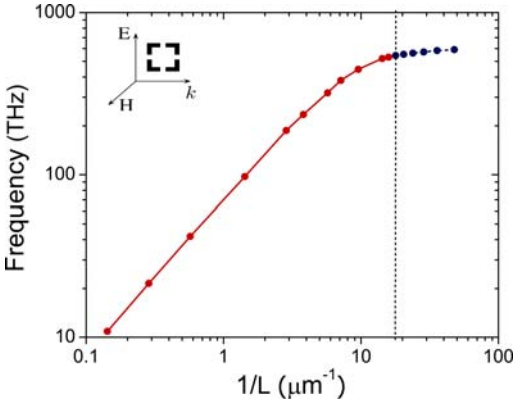

Fig. 8 (online colour at: www.pss-b.com) Scaling of the magnetic resonance frequency of the four-cut SRR with the inverse unit size is shown. The parameters of four-cut SRR are given by length $l = 0.914L$, width and thickness of the metal $w = t = 0.257L$ and gap-size $g = 0.05L$. The linear scaling $\omega_m \propto 1/L$ at low frequencies (large unit cells) breaks down at around 300 THz which is higher than that shown in Fig. 1. The blue solid circular symbol (right side of the vertical dotted line) indicate no $\mu < 0$ reached anymore.

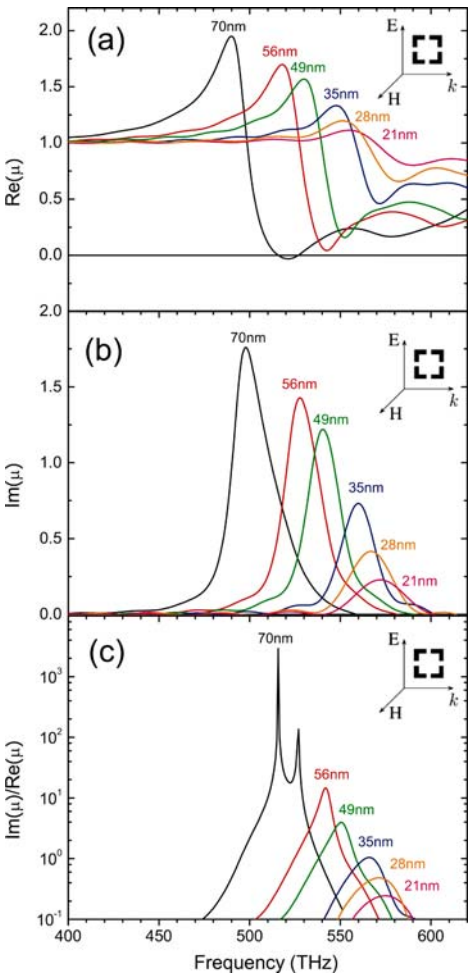

Fig. 9 (online colour at: www.pss-b.com) Real part (a) and imaginary part (b) of the resonant effective permeability $\mu(\omega)$ and loss tangent (c) $\mathrm{Im}(\mu(\omega))/\mathrm{Re}(\mu(\omega))$ are shown for a four-gap SRR as function of frequency for different sizes L of the SRR unit cell: $L = 70$ nm (black), 56 nm (red), 49 nm (green), 35 nm (blue), 28 nm (orange) and 21 nm (magenta). In part (a), the magnitude of magnetic resonance reduces as L scales down, and only $L = 70$ nm (black curve) shows a negative μ at around 520 THz. All the frequencies below 520 THz show negative μ.

moves to higher frequencies for smaller SRR size but slower as would be expected from linear scaling. Simultaneously, the strength of the resonance, and hence, the amplitude of the resonant $\mu(\omega)$, decreases. Notice that even at SRR sizes of 21 nm, there is a small resonance of μ, which is very weak so that μ does not reach negative values anymore. However, μ is still showing some structure and is not equal to one independent of frequency.

In Fig. 9b, the imaginary part of $\mu(\omega)$ is shown. Notice that as the size of the unit cell decreases, the width of the half-maximum of $\mathrm{Im}(\mu(\omega))$ increases, which means that the losses are getting larger as the size of the 4-cut SRR decreases. In addition the 4-cut design is favorable for more-dimensional materials not only for its highest attainable magnetic resonance frequency but also for its inherent symmetry. For a given structural size, the resonance frequency ω_{m} increases with the number of cuts, which brings the resonant refractive index n_{eff} closer in frequency to the edge of the Brillouin zone, $n_{\mathrm{BZ}} = \pi c/\omega L$, promoting periodicity artifacts [20, 21]. With the 4-cut design the resonance wavelength is comparable to the size of the unit cell and the effective medium theory ($\lambda \gg L$) is not obeyed anymore.

4 Conclusions

Using detailed numerical simulations we have systematically studied the scaling of the resonance frequency ω_{m} of single-cut and four-cut SRRs. For both cases, it is found that ω_{m} scales inversely propor-

tional to the size L of the unit cell of the SRR. For the single-cut SRR the linear scaling is obeyed up to 100 THz, while for the 4-cut SRR the scaling is obeyed up to 500 THz. Above these frequencies, ω_m saturates. The reason for the saturation is due to the increased kinetic inductance of the electrons (compared to the geometric inductance of the SRR ring). We found negative effective permeability up to 500 THz in the 4-cut SRR design. We have shown that the losses increase as the size of the SRR unit cell decreases. The saturation of the resonance magnetic frequency, as well as the losses, are responsible for the disappearance of the negative magnetic SRR response. Finally, we numerically calculated the current density, and the z-component of the magnetic field for SRRs at low and high frequencies. For high frequencies, the current density is non-zero in the whole metallic ring of the SRRs. This diamagnetic response can explain the derivation of $\mu(\omega)$ from unity which is observed at low and high frequencies.

Acknowledgments Work at the Ames Laboratory was supported by the Department of Energy (Basic Energy Sciences) under Contract No. DE-AC02-07CH11358. This work was partially supported by the AFOSR under MURI grant (FA9550-06-1-0337), by DARPA (Contract No. MDA-972-01-2-0016), EU FET projects Metamorphose and PHOREMOST, and by Greek Ministry of Education Pythagoras project. The research of C. M. Soukoulis is further supported by the Alexander von Humboldt Senior Scientist Award 2002.

References

[1] V. G. Veselago, Sov. Phys. Usp. **10**, 509 (1968).
[2] for recent review see, C. M. Soukoulis, M. Kafesaki, and E. N. Economou, Adv. Mater. **18**, 1941 (2006).
[3] R. A. Shelby, D. R. Smith, S. C. Nemat-Nasser, and S. Schultz, Appl. Phys. Lett. **78**, 489 (2001).
[4] D. Smith, W. Padilla, D. Vier, S. Nemat-Nasser, and S. Schultz, Phys. Rev. Lett. **84**, 4184 (2000).
[5] J. B. Pendry, Phys. Rev. Lett. **85**, 3966 (2000).
[6] J. Pendry, A. Holden, W. Stewart, and I. Youngs, Phys. Rev. Lett. **76**, 4773 (1996).
[7] J. Pendry, A. Holden, D. Robbins, and W. Stewart, IEEE Trans. Microw. Theory Tech. **47**, 2075 (1999).
[8] K. Aydin, K. Guven, M. Kafesaki, L. Zhang, C. M. Soukoulis, and E. Ozbay, Opt. Lett. **29**, 2623 (2004).
[9] C. G. Parazzoli, R. B. Greegor, K. Li, B. E. C. Koltenbah, and M. Tanielian, Phys. Rev. Lett. **90**, 107401 (2003).
[10] R. A. Shelby, D. R. Smith, and S. Schultz, Science **292**, 77 (2001).
[11] C. Enkrich, M. Wegener, S. Linden, S. Burger, L. Zschiedrich, F. Schmidt, J. F. Zhou, T. Koschny, and C. M. Soukoulis, Phys. Rev. Lett. **95**, 203901 (2005).
[12] N. Katsarakis, G. Konstantinidis, A. Kostopoulos, R. Penciu, T. Gundogdu, M. Kafesaki, E. Economou, T. Koschny, and C. M. Soukoulis, Opt. Lett. **30**, 1348 (2005).
[13] S. Linden, C. Enkrich, M. Wegener, J. F. Zhou, T. Koschny, and C. M. Soukoulis, Science **306**, 1351 (2004).
[14] T. J. Yen, W. J. Padilla, N. Fang, D. C. Vier, D. R. Smith, J. B. Pendry, D. N. Basov, and X. Zhang, Science **303**, 1494 (2004).
[15] N. Katsarakis, T. Koschny, M. Kafesaki, E. N. Economou, and C. M. Soukoulis, Appl. Phys. Lett. **84**, 2943 (2004).
[16] G. Dolling, C. Enkrich, M. Wegener, C. M. Soukoulis, and S. Linden, Opt. Lett. **31**, 1800 (2006).
[17] G. Dolling, C. Enkrich, M. Wegener, C. M. Soukoulis, and S. Linden, Science **312**, 892 (2006).
[18] J. F. Zhou, T. Koschny, L. Zhang, G. Tuttle, and C. M. Soukoulis, Appl. Phys. Lett. **88**, 221103 (2006).
[19] J. F. Zhou, L. Zhang, G. Tuttle, T. Koschny, and C. M. Soukoulis, Phys. Rev. B **73**, 041101 (2006).
[20] J. F. Zhou, T. Koschny, M. Kafesaki, E. N. Economou, J. B. Pendry, and C. M. Soukoulis, Phys. Rev. Lett. **95**, 223902 (2005).
[21] T. Koschny, P. Markos, E. N. Economou, D. R. Smith, D. C. Vier, and C. M. Soukoulis, Phys. Rev. B **71**, 245105-1–22 (2005).
[22] D. R. Smith, S. Schultz, P. Markos, and C. M. Soukoulis, Phys. Rev. B **65**, 195104 (2002).

